

## Ultrasound Features of Skeletal Muscle Can Predict Kinematics of Upcoming Lower-Limb Motion

M. HASSAN JAHANANDISH,<sup>1</sup> KAITLIN G. RABE,<sup>1</sup> NICHOLAS P. FEY,<sup>1,2,3</sup>  
and KENNETH HOYT <sup>1,4</sup>

<sup>1</sup>Department of Bioengineering, The University of Texas at Dallas, Richardson, TX 75080, USA; <sup>2</sup>Department of Mechanical Engineering, The University of Texas at Dallas, Richardson, TX, USA; <sup>3</sup>Department of Physical Medicine and Rehabilitation, UT Southwestern Medical Center, Dallas, TX, USA; and <sup>4</sup>Department of Radiology, UT Southwestern Medical Center, Dallas, TX, USA

(Received 30 April 2020; accepted 10 September 2020; published online 21 September 2020)

Associate Editor Thurmon E. Lockhart oversaw the review of this article.

**Abstract**—Seamless integration of lower-limb assistive devices with the human body requires an intuitive human-machine interface, which would benefit from predicting the intent of individuals in advance of the upcoming motion. Ultrasound imaging was recently introduced as an intuitive sensing interface. The objective of the present study was to investigate the predictability of joint kinematics using ultrasound features of the rectus femoris muscle during a non-weight-bearing knee extension/flexion. Motion prediction accuracy was evaluated in 67 ms increments, up to 600 ms in time. Statistical analysis was used to evaluate the feasibility of motion prediction, and the linear mixed-effects model was used to determine a prediction time window where the joint angle prediction error is barely perceivable by the sample population, hence clinically reliable. Surprisingly, statistical tests revealed that the prediction accuracy of the joint angle was more sensitive to temporal shifts than the accuracy of the joint angular velocity prediction. Overall, predictability of the upcoming joint kinematics using ultrasound features of skeletal muscle was confirmed, and a time window for a *statistically* and *clinically* reliable prediction was found between 133 and 142 ms. A reliable prediction of user intent may provide the time needed for processing, control planning, and actuation of the assistive devices at critical points during ambulation, contributing to the intuitive behavior of lower-limb assistive devices.

**Keywords**—Ultrasound imaging, Skeletal muscle, Motion prediction, Human-machine interface.

## INTRODUCTION

Approximately 11.4% of the world population—an estimated 877 million people—face moderate to extreme difficulty with their daily mobility.<sup>50</sup> Lower-limb assistive devices hold the promise to enhance activity and community involvement of this population.<sup>6,33</sup> However, effective human-device integration is still limited by the lack of a reliable interface between the user and the device.<sup>15,44</sup> For instance, 30–40% of the individuals who use lower-limb prostheses expressed difficulty in controlling their device.<sup>19,44</sup> To address this issue, assistive devices need to accurately infer and adapt to the intent of the user and demonstrate an intuitive behavior.

Ultrasound imaging was recently introduced as a sensing interface to serve as a means for the users to intuitively convey their intention to the assistive device. Ultrasound is a noninvasive sensing modality that measures the deformation of deep and superficial muscle tissue in real-time.<sup>16</sup> The high spatiotemporal resolution and specificity that are inherent to the ultrasound measurements of muscle deformation<sup>16,30</sup> have enabled researchers to infer fine volitional motor tasks such as finger movements and dexterous control of robotic hands.<sup>2,8,20,51</sup> Ultrasound technology has further been used to estimate and predict the non-weight-bearing volitional motion of the knee and ankle joints, as well as identify the phases during a gait cycle.<sup>24–26,36,53</sup> Most recently, Rabe *et al.* used transverse ultrasound images of lower-limb skeletal muscles for continuous estimation of knee angular velocity as

Address correspondence to Nicholas P. Fey, and Kenneth Hoyt, Department of Bioengineering, The University of Texas at Dallas, Richardson, TX 75080, USA. Electronic mails: nicholas.fey@utdallas.edu, kenneth.hoyt@utdallas.edu

Nicholas P. Fey and Kenneth Hoyt share co-senior responsibilities over this work.

well as estimation of the hip, knee, and ankle moments during varying modes of ambulation.<sup>37,38</sup>

The real-time control responsiveness, which calls for a minimal amount of controller delay, is essential for the effective functioning of an assistive device. Amplitude-based controllers for myoelectric upper-limb prostheses can tolerate control delays smaller than 100 ms.<sup>14</sup> Smith *et al.* investigated the effect of controller delay and window length for a pattern recognition-based myoelectric controller operating a virtual upper-limb prosthesis and determined an optimal window length between 150 and 250 ms where the users have better control over the virtual prosthesis.<sup>42</sup> For the lower-limb prostheses that utilize a pattern-recognition control scheme, a safe time window has been shown to exist that can be used to switch between ambulation modes without compromising the stability of the user.<sup>52</sup> More recently, Simon *et al.* demonstrated that delaying ambulation mode transition decisions by 90 ms contributes to improved control of a powered transfemoral prosthesis.<sup>41</sup>

While it appears that assistive devices can tolerate a certain amount of delay, an assistive device that is actuated as a result of physiological signals of the user must provide a quick response to the neuromuscular signals while maintaining performance. Intuitive interfaces (e.g. surface electromyography (sEMG), ultrasound, etc.) can recognize the neuromuscular signals before the initiation of motion,<sup>5,9,49</sup> therefore they are expected to precede the motion. Ultrasound imaging is capable of accessing kinematic and kinetic features of the skeletal muscle.<sup>16,30</sup> For instance, ultrasound echogenicity is a kinetic feature of the muscle that reflects the ongoing formation of cross-bridges during motor unit recruitment and before the production of muscle force.<sup>9,10,24</sup> Kinematic features of the muscle that are visualized by ultrasound signals (e.g. muscle thickness, pennation angle, etc.) undergo a change during sarcomere shortening, when the muscle force overcomes the muscle segment inertial forces, and before the initiation of the joint motion.<sup>9,30</sup> While kinetic and kinematic ultrasound features of the muscle exhibit their change at various stages during muscle excitation-contraction, they all precede the joint motion. Hence, ultrasound features of the skeletal muscle may be used to predict the upcoming joint motion, toward enhancing the real-time control responsiveness of assistive devices.

The objective of the present study was twofold: (1) to investigate the feasibility for a reliable prediction of the kinematics of upcoming joint motion, using the ultrasound features of lower-limb skeletal muscle, and (2) to characterize the amount of time that the ultra-

sound features of muscle precede the joint motion during non-weight-bearing knee extension/flexion experiment. We *hypothesize* that ultrasound features of the proximal skeletal muscle precede the distal joint movements, and therefore, can provide a reliable source of information to predict the upcoming joint motion.

## MATERIALS AND METHODS

### Subjects and Experiment

Nine able-bodied subjects (5 males and 4 females with a mean age of  $26.2 \pm 12.6$  years) completed a non-weight-bearing knee extension/flexion experiment. Subjects were recruited without bias of race or gender. Subjects with significant arthritis or other joint problems, neuromuscular disorders, cognitive deficits or visual impairments that would impair their ability to follow simple instructions during the experiments, and co-morbidity that interferes with the study (e.g., stroke, pacemaker placement, severe ischemia, cardiac disease, etc.) were excluded during the recruitment.

While seated, participants were instructed to fully extend their knee joint and flex it back to the rest position at a self-selected pace. The movement was repeated three times for each leg with 30 s of rest between repetitions. Participants were equipped with a custom 3D printed ultrasound transducer holder placed approximately 60% of the distance from the anterior superior iliac spine to the proximal base of the patella. The ultrasound transducer was securely placed longitudinally over the rectus femoris (RF) muscle and images were captured using a handheld and wearable ultrasound scanner (mSonic, Lonshine Technologies Inc, Beijing, China). This system was modified by the manufacturer to support an extended ultrasound image acquisition (1024 frames). Traditional grayscale (i.e. brightness-modulated, B-mode) ultrasound images were collected in real-time using a transmit frequency of 7.5 MHz and a dynamic range of 50 dB. A PS-2137 wireless electrogoniometer (Pasco, CA, USA) with an accuracy of  $\pm 1^\circ$  and a resolution of  $0.1^\circ$  was used to measure the knee angle during the movement. Data from the electrogoniometer was recorded wirelessly on a smartphone in real-time. The experimental setup is shown in Fig. 1. The International Conference on Harmonisation of Good Clinical Practice (ICH-GCP) guidelines were followed for the experiment.<sup>11</sup> The experiment protocol was approved by the Institutional Review Board (IRB) at the University of Texas at Dallas and all the participants provided informed written consent.

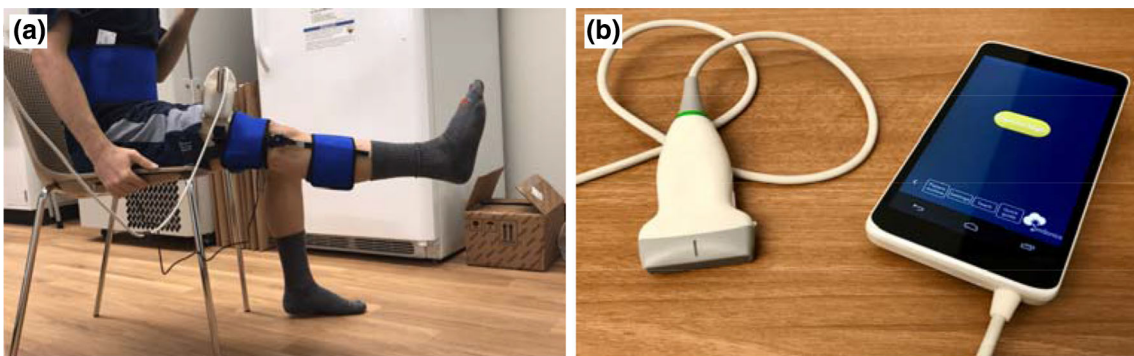


FIGURE 1. (a) Experimental setup on a human subject and, (b) the handheld ultrasound system used for muscle imaging.

### Methods

A multiscale ridge filter along with a random sample and consensus (RANSAC) model<sup>24</sup> were used to automatically segment five ultrasound image-derived features of the RF muscle during motion including (1) muscle thickness, (2) angle between aponeuroses, (3) pennation angle, (4) fascicle length, and (5) echogenicity. Each ultrasound image sequence was processed using the feature segmentation method to produce a time-series for each of the five features. To estimate the knee joint angle, a regression-based machine learning approach was utilized to generate continuous motion estimation data. Ultrasound features were used as predictors and Gaussian process regression (GPR) models with quadratic kernels were trained to estimate knee joint angle and angular velocity as the response.<sup>39</sup> A nested cross-validation scheme was utilized for feature selection and validation of the regression machine learning models. Motion estimation error was calculated during the validation process by the root mean square error (RMSE) between the estimated motion time-series  $\hat{y}_t$ , and the measured time-series  $y_t$  by the electrogoniometer on the knee joint.

A series of temporal shifts ( $T_s$ ) was introduced to evaluate the feasibility of predicting the kinematics of upcoming lower-limb motion. The instantaneous values of ultrasound features at a certain point in time  $t$  were used to train the GPR models to predict the kinematics of joint motion at a future time point  $t + T_s$  based on a temporal shift  $T_s$ . The temporal shifts ranged from  $T_s = 0$  ms to  $T_s = 600$  ms with a temporal step size of 67 ms, where  $T_s = 0$  ms corresponds to the original motion estimation (i.e. no prediction, Fig. 2a). The process of predicting motion in time using the ultrasound features of a certain time point is illustrated in Fig. 2b, where the solid lines indicate a  $T_s = 0$  ms and dashed lines a  $T_s = 600$  ms, i.e. prediction of the motion profile 600 ms ahead of time.

### Statistical Analysis and Evaluation

The accuracy of motion predictions was evaluated by calculating the RMSEs of the predicted time-series of knee joint kinematics  $\hat{y}_{t+T_s}$  with reference to the joint motion time-series recorded by the electrogoniometer  $y_{t+T_s}$ . To assess the effect of the temporal shifts on the quality of motion prediction, the RMSEs of the motion predictions were analyzed using a repeated-measures analysis of variance (ANOVA) test.<sup>23</sup> It was anticipated that the motion prediction accuracy loses its reliability at some point in time. Therefore, multiple posthoc comparisons of the RMSEs were performed to compare the RMSEs of motion predictions to the RMSE of motion estimation and find out whether there was a significant change in motion prediction error compared to motion estimation error. The  $p$ -values were adjusted using a Bonferroni correction for multiple comparisons.

To further examine the effect of the temporal shifts on the prediction of the joint kinematics at each point throughout the motion, Statistical Parametric Mapping (SPM) was used. SPM is an expansion of the conventional statistical tests that enables the statistical comparison of an entire 1D (e.g. trajectories) or 2D (e.g. images) dataset rather than specific features extracted from the data.<sup>34,35</sup> Therefore, SPM can be employed to analyze an entire trajectory of joint motion rather than single features of it such as RMSE, while simultaneously controlling for multiple comparisons and the dependency between the adjacent time points. In the present study, we used the temporal shifts as the fixed effect and SPM ANOVA was used to analyze whether there are certain points during the motion where the prediction accuracy is significantly affected by increasing the temporal shifts. The analysis was done separately for the predicted joint angle and angular velocity trajectories and the  $p$ -values were adjusted using a Bonferroni correction for pairwise comparison of the predicted trajectories.

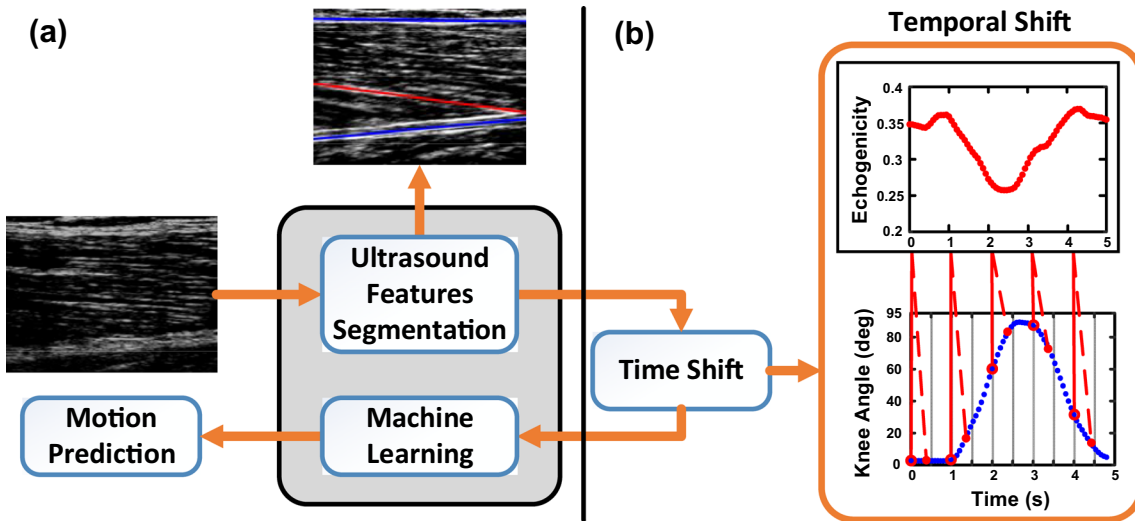


**FIGURE 2.** Overview of the motion prediction framework while introducing the temporal shifts between the ultrasound features of muscle and the joint motion. Panel (a) shows the original motion estimation and panel (b) illustrates the process of introducing the temporal shifts where the dashed lines show a temporal shift of 600 ms that results in the prediction of upcoming motion compared to the solid lines that produce the original estimation.

The linear mixed-effects model was used to find a model that best explains the motion prediction RMSE data and to identify the amount of temporal shift that can produce a clinically meaningful difference (CMD) in the prediction accuracy. It has been reported that the sensitivity of able-bodied humans to the external passive changes in their knee joint position, which is measured by the Threshold to Detection of Passive Motion (TDPM) test, ranges between 1.07° and 2.7° with a mean sensitivity of 1.76°.<sup>4,18,29,40</sup> The mean sensitivity value of 1.76° was used as a CMD along with the linear mixed-effects model to find out the maximum amount of temporal shift that can cause a change in the motion prediction accuracy that is still not perceivable by the user.

The relationship between the RMSEs of motion prediction and the temporal shifts was determined using a linear mixed-effects model which is expressed as

$$y = X\beta + Zu + \varepsilon \quad (1)$$

where  $y$  is a vector of outcome variables,  $X$  is the matrix of the fixed-effects,  $\beta$  is a vector of fixed-effects regression coefficients,  $Z$  is the design matrix for the random-effects that account for inter-subject variabilities,  $u$  is the vector of the random-effects parameters, and  $\varepsilon$  is a vector of residual errors.<sup>32</sup> The prediction RMSEs were the outcome variables, the temporal shift values were the fixed-effect variables, and the subject was defined as the random-effect variable. A maximum likelihood method was used to find the best fit for the motion prediction RMSE data based on the temporal shifts and the subject variabilities. The null hypothesis

was that  $\beta$  (i.e. the regression coefficient for temporal shifts) and  $u$  (i.e. the random-effect parameter) were zero. The RMSE of ultrasound-based prediction was used as  $y$  for each temporal shift  $\beta$  in (1) to calculate the coefficients  $X$  and  $Z$ . Then, the model that was fit to the ultrasound data was used along with the value of the knee joint TDPM test that was replaced as a new  $y$ . The new  $y$  in Eq. (1) was then used to identify a value for  $\beta$  that is an amount of temporal shift that can cause a clinically meaningful (i.e. perceivable) change in prediction accuracy of the upcoming joint motion compared to the estimation accuracy.

## RESULTS

### *Prediction of the Upcoming Motion*

Nine able-bodied subjects performed a knee extension/flexion movement at a self-selected speed while seated in a chair. The mean (SD) time frame for each part of the motion is as follows, knee extension: 2.06 (0.56) s, knee flexion: 2.57 (0.71) s, and the total length of knee extension/flexion: 4.63 (1.02) s. Figure 3 shows the time course of the recorded knee angle and angular velocity for a sample subject along with the predicted trajectories for the 200 ms and 600 ms temporal shifts. The average RMSE of the predicted trajectories for the knee joint angle and angular velocity with reference to the recorded motion kinematics are presented in Tables 1 and 2, respectively. The RMSE values of the predicted trajectories were further normalized with respect to the RMSE of the original estimation (i.e. the 0 ms temporal shift) to highlight the change in the

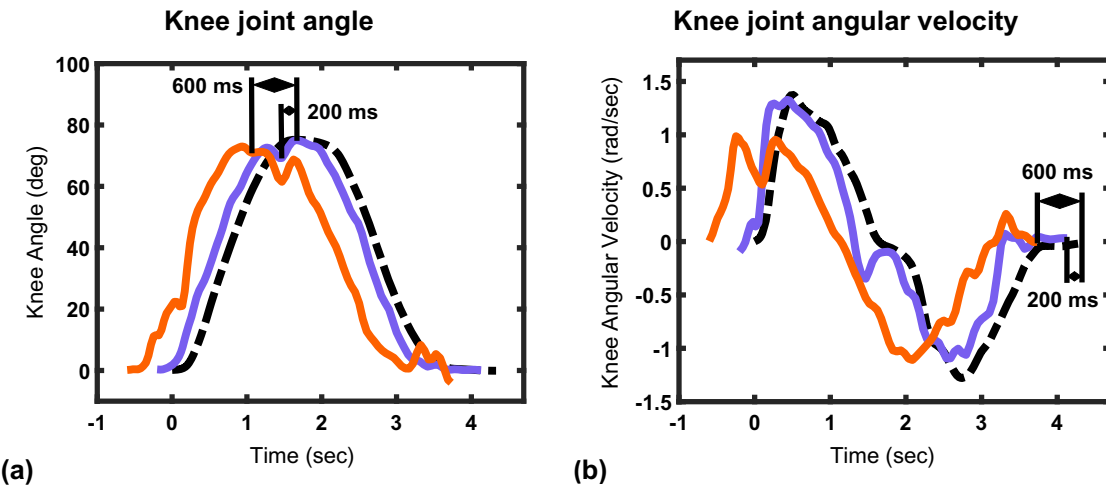


**FIGURE 3.** Time course of the recorded joint kinematics (dashed black lines) for a sample subject. The predicted trajectories of (a) the knee angle and (b) the knee angular velocity are shown for two representative temporal shifts of 200 ms (solid blue line) and 600 ms (solid orange line) as a function of time. The marks shown in (a) represent the maximum knee extension points and the time precedence of the predicted trajectories.

**TABLE 1.** RMS error for knee joint angle prediction averaged across subjects ( $N = 9$ ).

Temporal shift (ms)	0	67	133	200	267	334	400	467	533	600
Mean RMSE (deg)	7.39	7.91	8.59	8.98	9.47	10.19	10.08	10.42	10.87	11.34
SD RMSE (deg)	2.91	3.02	3.09	3.12	3.36	3.45	3.43	3.49	3.36	3.92

**TABLE 2.** RMS error for knee angular velocity prediction averaged across subjects ( $N = 9$ ).

Temporal shift (ms)	0	67	133	200	267	334	400	467	533	600
Mean RMSE (rad/s)	0.258	0.254	0.249	0.240	0.237	0.241	0.248	0.250	0.254	0.257
SD RMSE (rad/s)	0.053	0.057	0.052	0.053	0.062	0.065	0.070	0.086	0.093	0.105

accuracy of the motion prediction that is caused by the temporal shift. The mean and the 95% confidence interval (CI) of the normalized changes in prediction errors are shown in Figs. 4a and 4b for the prediction of joint angle and angular velocity, respectively. The prediction accuracy of the joint angle was affected by the amount of temporal shift where a linearly increasing trend ( $R^2 = 0.97$ ) was observed for the change of the prediction error as the temporal shift increases (Fig. 4a; Table 1). On the other hand, the prediction of the joint angular velocity was trending toward a 2nd-order polynomial ( $R^2 = 0.83$ ) where the prediction error decreases up to a certain point and then starts to increase as the temporal shift increases. The time length of the knee extension/flexion movement did not show any significant effect on the accuracy of predictions or the rate of change of the prediction accuracy with respect to the temporal shifts.

The result of a repeated-measures ANOVA test supports the increasing trend that the temporal shifts had a significant effect on the knee angle prediction ( $p < 0.001$ ). However, multiple comparisons of the joint angle prediction errors revealed that the prediction errors did not change significantly between the estimation and the temporal shifts smaller than 200 ms ( $p > 0.05$ , Table 3). Statistical analysis of the joint angular velocity predictions exhibited that the temporal shifts did not have a significant main effect on the velocity predictions ( $p = 0.60$ ). Furthermore, the posthoc comparisons unveiled that a temporal shift of 133 ms produced a significant decrease in the prediction error of the angular velocity ( $p = 0.03$ ), Table 4. All statistically-significant findings were observed with an effect size of  $> 0.62$  (CI 0.52–1.31), which covers the range of a medium to very large effect size. Based on these results, the joint angle was predictable up to

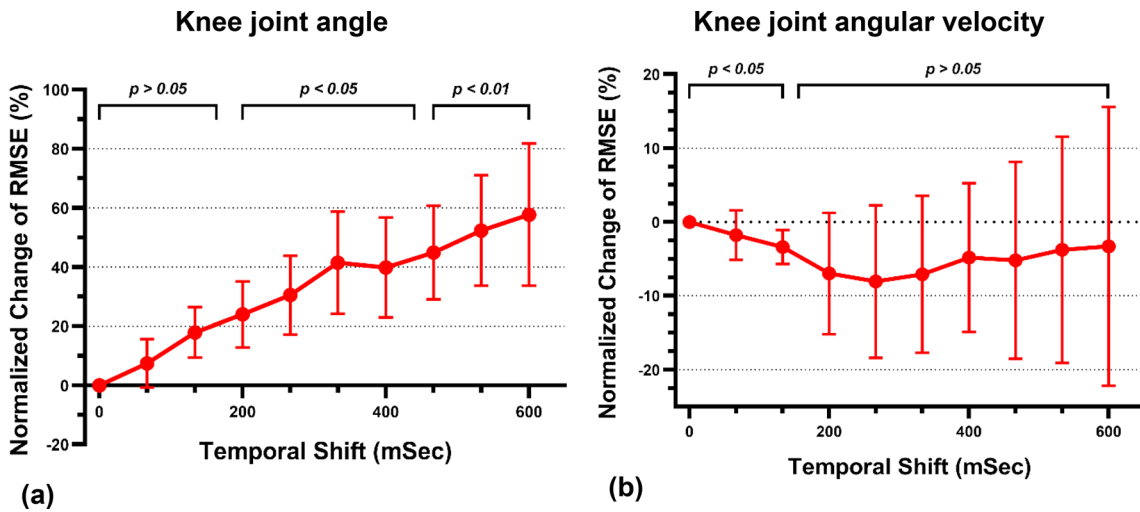


FIGURE 4. The normalized change (%) of the prediction error compared to the estimation error that is caused by the temporal shift, for the prediction of (a) knee joint angle, and (b) knee joint angular velocity. The  $p$ -values are the result of pairwise comparisons performed after ANOVA tests. Note that the ordinate scales differ between (a) and (b).

TABLE 3. The  $p$ -values for the pairwise comparison of the knee angle predictions.

	67	133	200	267	333	400	467	533	600
0	1.00	0.06	<b>0.05</b>	<b>0.04</b>	0.03	0.03	0.01	0.01	0.03
67		0.59	0.16	0.10	<b>0.03</b>	<b>0.05</b>	<b>0.03</b>	<b>0.05</b>	<b>0.05</b>
133			0.80	0.19	0.06	<b>0.03</b>	<b>0.04</b>	0.07	0.20
200				0.29	<b>0.03</b>	<b>0.03</b>	<b>0.03</b>	0.07	0.28
267					0.27	0.15	0.31	0.30	0.96
333						1.00	1.00	1.00	1.00
400							1.00	1.00	1.00
467								1.00	1.00
533									1.00

Bold value indicates statistical significance ( $p < 0.05$ ).

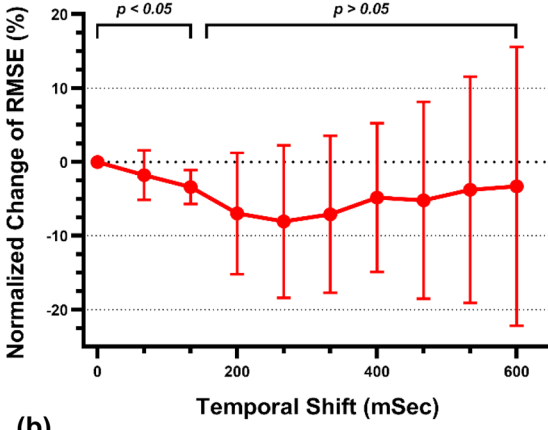
TABLE 4. The  $p$ -values for the pairwise comparison of the knee velocity predictions.

	67	133	200	267	333	400	467	533	600
0	0.58	<b>0.03</b>	0.36	0.44	0.58	0.84	0.93	0.99	1.00
67		0.74	0.52	0.62	0.96	1.00	1.00	1.00	1.00
133			0.84	0.85	0.99	1.00	1.00	1.00	1.00
200				1.00	1.00	1.00	1.00	1.00	1.00
267					1.00	0.98	1.00	1.00	1.00
333						0.97	1.00	1.00	1.00
400							1.00	1.00	1.00
467								0.97	1.00
533									1.00

Bold value indicates statistical significance ( $p < 0.05$ ).

200 ms in time with no significant degradation of the prediction accuracy, and predicting the joint angular velocity with a time precedence of 133 ms exhibited a significantly higher accuracy. These findings suggest that there is an optimal time window between 133 and 200 ms for predicting the kinematic parameters of the

### Knee joint angular velocity



upcoming knee joint motion based on ultrasound features of the skeletal muscle.

### Analysis of the Predicted Motion Trajectories

SPM is a method that provides a detailed statistical analysis of 1-D trajectories. Here it was used to extend the results of the ANOVA tests and find out whether the effect of temporal shifts on the predicted motion trajectories was limited to certain points during the motion or if it has a broad impact on the entire trajectory of motion. Figure 5 displays the SPM statistics that highlight the regions of the trajectories during the motion progression that are significantly affected by increasing the temporal shifts. Since time-normalized trajectories were used to produce the SPM results, 0–50% of the motion progression in Fig. 5 represents the knee extension and 50–100% represents the knee flexion. There were three distinct peaks in the SPM statistics for the joint angle prediction that show the points during motion where the prediction accuracy was significantly affected by the temporal shift (28–30% of the motion progression,  $p = 0.04$ ; 45–57% of the motion progression,  $p < 0.001$ ; 98–100% of the motion progression,  $p = 0.03$ ), Fig. 5a. The highest peak existed when the joint was changing direction from extension to flexion (45–57% of the motion progression,  $p < 0.001$ ), revealing that the temporal shifts had the highest impact on the prediction of the joint angle when the joint was changing direction, Fig. 5a. The SPM analysis of the predicted trajectories of the angular velocity showed less sensitivity to the temporal shifts and resulted in identifying two regions in the motion trajectory where the accuracy of the

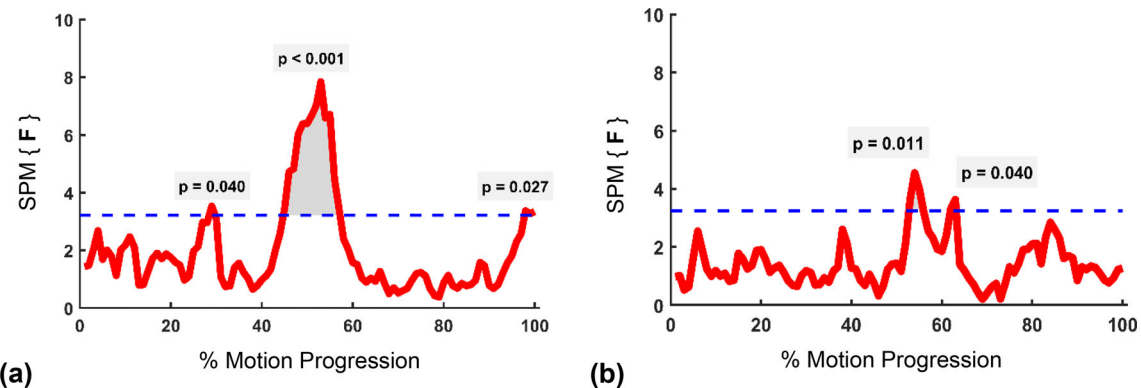


**FIGURE 5.** SPM ANOVA results for the (a) knee angle and, (b) knee angular velocity prediction showing the points during the knee extension/flexion movement where the prediction is significantly affected by the temporal shift. The SPM F-statistics is shown as a function of the motion progression. 50% motion progression refers to full extension.

prediction significantly changed with increasing the temporal shift (53–56% of the motion progression,  $p = 0.01$ ; 61–63% of the motion progression,  $p = 0.04$ ), Fig. 5b. Noteworthy, the highest peak was again located right after the joint changed direction (53–56% of the motion progression,  $p = 0.011$ ), showing that the most sensitive point to increasing the temporal shifts was when the joint was changing direction during the motion, regardless of the kinematic parameter that was being predicted, Fig. 5b. Since switching between the swing and stance phases of the gait is where the direction of the joint motion changes, this observation could potentially be very meaningful for device implementation of an ultrasound-based predictive approach when translated to weight-bearing tasks such as walking.

The representative trajectories of the predicted joint motion are shown in Fig. 6 for the original motion estimation (temporal shift = 0 ms), the 200 ms, and the 600 ms conditions along with the recorded trajectories by the electrogoniometer on the knee joint. As informed by the ANOVA and SPM tests, both 200 ms and 600 ms trajectories for joint angle prediction presented a less accurate fit with respect to the recorded motion trajectory than the original estimation trajectory, Figs. 6a–c. It is visually apparent that the 600 ms trajectory did not provide an acceptable fit to the recorded trajectory, whereas the 200 ms condition seemed to have a better fit, Figs. 6b–c. In contrast, Figs. 6d–f highlight that the 200 ms trajectory had a better fit to the recorded trajectory of the joint angular velocity compared to both the estimation (i.e. 0 ms) and the 600 ms trajectories.

#### Linear Mixed-Effects Model

In addition to the previous results that measured the presence of a *statistical* difference in the motion pre-

diction accuracy with respect to temporal shifts, a linear mixed-effects model was constructed to determine the presence of a *clinically* significant change in motion prediction accuracy as the temporal shift increases.

The results of the linear mixed-effects model for the angle prediction indicated that both temporal shift ( $\beta = 0.0066$ ,  $p < 0.001$ ) and inter-subject variability ( $p < 0.05$ ) had a significant effect on the motion prediction error. The model coefficients allowed us to calculate that a  $1.76^\circ$  (i.e. the value of the knee joint TDPM test) change in prediction error will be obtained with a mean temporal shift of 248 ms. Since the 248 ms was the mean value obtained from the model, it represents the amount of temporal shift required to cause a change in prediction error that is “barely perceivable” for 50% of the subjects. A more conservative estimate of the temporal shift was obtained such that it would produce a change in prediction error not perceivable to 90% of the population (mean + 1.645 SD). This conservative estimate showed that a temporal shift of 142 ms would generate a change in prediction error that would not reach the  $1.76^\circ$  and, therefore, would not be perceivable for 90% of the population. These findings narrow the time window to between 133 and 142 ms for a *statistically* and *clinically* reliable prediction of the upcoming joint kinematics based on ultrasound features of the muscle.

## DISCUSSION

Ultrasound features of the skeletal muscle are neuromuscular signals, derived from muscle activation and contraction,<sup>9</sup> and are expected to precede the joint movement. In the present study, we assessed the hypothesis that ultrasound features of the skeletal muscle precede the joint motion, and therefore, are

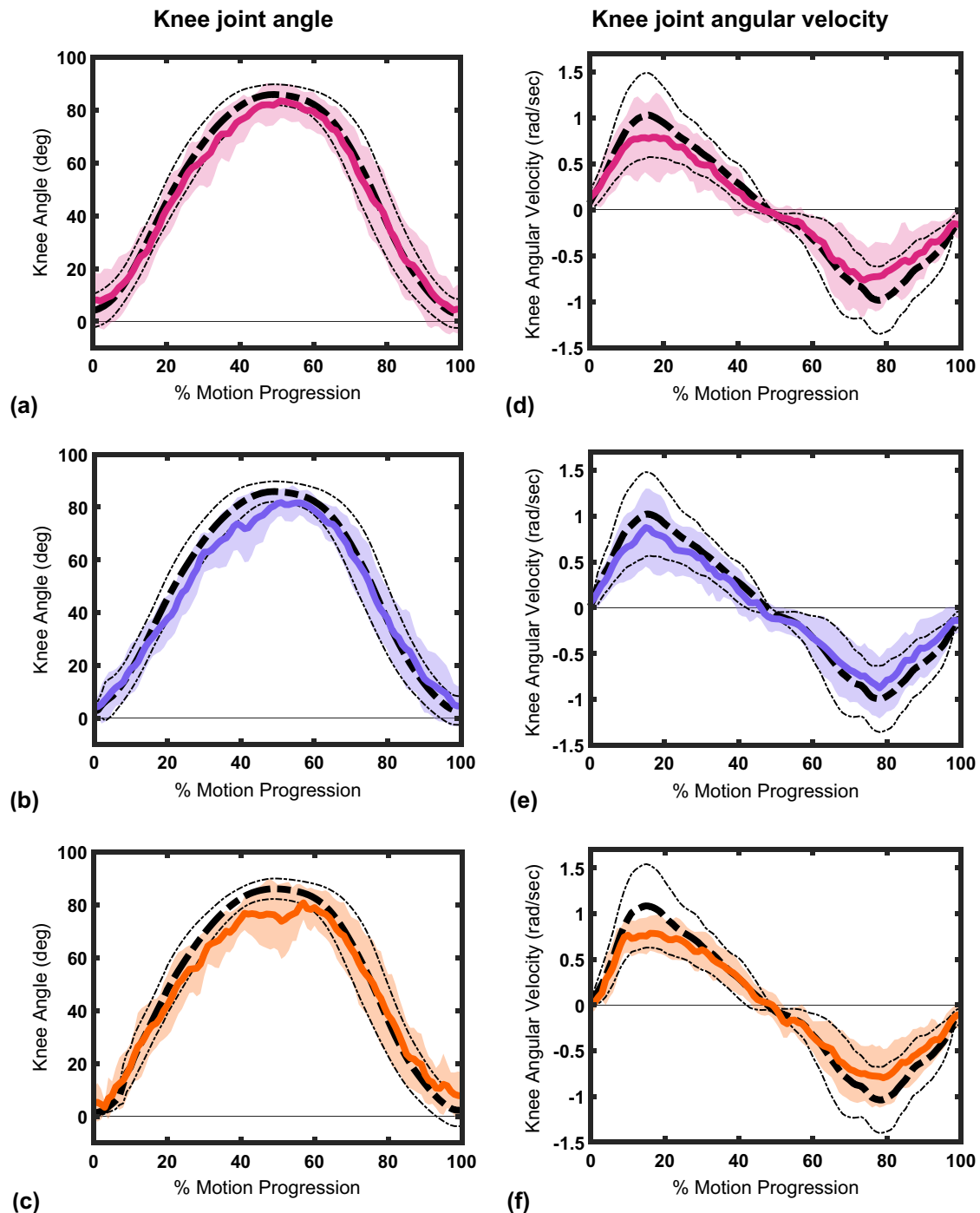


**FIGURE 6.** The trajectories of the joint kinematics as a function of motion progression for three representative temporal shifts including (a, d) 0 ms, i.e. original estimation, (b, e) 200 ms, (c, f) 600 ms. The dashed black lines show the recorded trajectories and the solid colored lines show the predicted trajectories. The trajectories are averaged across all subjects and the shaded areas represent mean  $\pm 1$  SD.

useful to predict the kinematics of upcoming lower-limb movements. Further, the temporal precedence of the ultrasound features to the motion was characterized and a time window was found for reliable prediction of the upcoming joint motion during non-weight-bearing knee extension/flexion.

The findings of the present study demonstrate the feasibility of predicting the kinematics of upcoming lower-limb joint motion using ultrasound features of skeletal muscle. While the prediction of joint angle was *statistically* reliable up to 200 ms, the prediction of joint angular velocity showed higher robustness to the

temporal shift with a statistically significant enhancement in the prediction accuracy for the 133 ms condition. Inspecting each row of Table 3 shows that the joint angle prediction accuracy did not differ between the conditions with temporal shifts larger than 200 ms. This indicates that the variability increased between subjects and the prediction was not reliable. The only temporal shift with a significant difference compared to the original estimation was the 133 ms (see Table 4), showing that enhanced prediction accuracy may not be achieved beyond 133 ms. SPM statistics revealed that the temporal shift only had a significant effect on the prediction of the joint angular velocity around 50% of motion progression. However, increasing the temporal shift seems to also impact the quality of fit of the predicted trajectories to the recorded trajectory around the 20% and 80% points during motion progression (Figs. 6d–f). This observation can be explained with the reduced sensitivity of SPM as a result of increased variability in the dataset.

Higher predictability of the joint angular velocity indicates that the joint angle has temporal precedence to the joint angular velocity in relation to the ultrasound features. This is a surprising observation and suggests that different driving factors might dominate the intramuscular mechanisms producing the two kinematic parameters of movement. The joint angle is not only a function of active motion but also a function of posture. The tonic muscles that are responsible for maintaining posture have a higher density of slow-twitch fibers.<sup>43</sup> These fibers have a lower activation threshold<sup>21</sup> and activate earlier than fast-twitch fibers, which likely is revealed in ultrasound image patterns. Conversely, producing angular velocity requires active motion, which needs the contribution of the fast-twitch muscle fibers with a higher activation threshold.<sup>21,43</sup> Due to the late activation of fast-twitch fibers, alteration of the ultrasound signal caused by the production of the joint velocity would lag the change in the ultrasound signal that is caused by the generation of the joint angle. From a mechanical perspective, it makes intuitive sense as the generation of active motion would require the active muscle force to first overcome the inertia of muscle-tendon units,<sup>31,46</sup> which introduces a time delay.

Our results indicate that a reliable prediction of the joint motion is possible within a time window of 133–142 ms, which agrees well with the results of similar studies performed on myoelectric prosthetic hands.<sup>14,42</sup> Koch *et al.* used the sEMG signals of the forearm muscles for the early prediction of hand movements using a recurrent neural network. Their work demonstrated the predictability of hand movements up to 200 ms, as well as the contribution of incorporating the time history of the sEMG signals.<sup>28</sup> Farmer *et al.*

successfully used a nonlinear autoregressive model for continuous prediction of prosthetic ankle angle in three transtibial amputees using within-socket myoelectric recordings, up to 150 ms.<sup>13</sup>

While sEMG signals are believed to reflect muscle excitation which precedes muscle contraction, our results tightly match the sEMG-based studies. This agreement can be explained by the penetration depth of ultrasound in muscle tissue, which can take advantage of the onset of motor unit recruitment. Ultrasound image intensity is a feature that has been suggested to reflect an intramuscular process<sup>9,10</sup> shown by the rapid change of hyperechoic and hypoechoic interfaces which is associated with muscle excitation.<sup>10</sup> Furthermore, due to the larger portion of low-threshold slow-twitch muscle fibers in the deeper regions of muscle,<sup>12,27</sup> the activation of deep muscle tissue precedes the activation of superficial muscle tissue.<sup>9,21</sup> Considering that sEMG lacks access to deep muscle tissue signals, the high-resolution penetration that ultrasound provides to deep tissue structures (e.g. the field of view in ultrasound images used in the present study was 6–7 cm) is likely a significant contributing factor to achieve comparable estimates with sEMG. Begovic *et al.* reported that the electromechanical delay (i.e. the time delay between onset of muscle fiber motion and the force production) detected by ultrasound is  $49.7 \pm 7.0$  ms during voluntary contraction of quadriceps femoris muscles.<sup>5</sup> Given the anticipated delay between the onset of force production and the joint movement, 133–142 ms seems like a realistic estimate of a reliable time window for motion prediction.

Statistical analysis of the prediction errors showed whether there was a difference between the prediction accuracies for different temporal shifts. However, it did not inform whether the difference was of any practical importance. The sensitivity of humans in perceiving the position of their limb (i.e. kinesthesia), has been studied in psychophysiology and neuroscience research. Among different tests developed to examine knee kinesthesia, TDPM is the most established and reliable test that attempts to find the sensitivity of humans to passive joint motion.<sup>1,18</sup> Different studies report the knee joint TDPM to range between 1.52 and 2.70°.<sup>4,18,29,40</sup> We defined the average reported value for the knee joint TDPM (i.e. 1.76°) as a CMD in the prediction accuracy that can be perceived by the user. We used the linear mixed-effects model to determine an amount of temporal shift that can produce a change in joint angle prediction error that is equivalent to the knee joint TDPM (i.e. 142 ms), hence barely perceivable by 90% of the sample population. It would have been interesting to perform this type of analysis for the angular velocity prediction. There are no CMD data

for angular velocity in the literature to be used with the linear mixed-effects model, therefore, more investigations are needed to incorporate user perception of joint angular velocity.

It has been shown that it takes around 90 ms after an ambulation mode transition event for discriminating patterns to emerge in the mechanical signals recorded by the sensors on a powered transfemoral prosthesis.<sup>41</sup> Since the mechanical signals are a result of the movement, they are always delayed compared to the motion. Our results demonstrate that ultrasound features of the muscle allow for reliable prediction of the motion up to 142 ms in advance. This will provide a time window for processing, control planning, and actuation, hence improving the safety and volitional behavior of the device. For instance, the timing of knee flexion and knee-lock during gait is essential to ensure the safety of the user.<sup>49</sup> From a practical standpoint, a reliable prediction might play an important role in a real-world situation where the device needs to adapt to a continuously varying terrain, and a late knee-lock or an early knee flexion might lead to a knee collapse which might result in a fall.

sEMG has been used as a noninvasive intuitive interface for human motion estimation<sup>7,47</sup> and assistive device control.<sup>42,44</sup> However, ultrasound imaging has several advantages that might prove useful for volitional control of assistive devices, including higher dimensionality and resolution of ultrasound data, higher penetration depth that provides access to deep muscle tissue, and the specificity of ultrasound signals. Moreover, the present work showed promising results demonstrating the predictive capability of instantaneous values of ultrasound features during a volitional movement. Recent efforts toward miniaturization of ultrasound technology have led to several designs for low-profile wearable transducers that include miniaturized sensors as flexible substrates.<sup>3,17</sup> The combination of miniaturization of ultrasound sensing and the predictive capability for continuous prediction of volitional movements demonstrates the potential for ultrasound as a viable intuitive interface for human motion prediction and assistive device control.

#### Limitations and Future Work

The focus of the present work was to study the timing of the ultrasound features and investigate the predictability of joint motion. However, our current results are limited to a non-weight-bearing motion which is performed relatively slowly compared to daily activities. The model allowed for a prediction window that covers around 10% of the time frame of the flexion or extension movements. However, the prediction time frame would have to adapt to ambulatory

activities that usually happen at a faster pace for practical use in lower-limb assistive devices. Since the rate of motor unit recruitment during muscle activation depends on the locomotion task,<sup>22,45</sup> it would not be surprising to find a different time window for optimal prediction of motion during different dynamic tasks. Therefore, characterizing the model prediction time frame within the time frame of each activity would be an interesting direction for future work. Specifically, it would be very interesting to study the feasibility of predicting the upcoming transition points between different modes when ambulating on a continuously varying surface. Although it will be challenging to predict those events, it will likely have a great impact on the intuitiveness of assistive devices for better adaptation to the user's intent and the environment. To that end, the time history of ultrasound features coupled with predictive models (such as RNNs or autoregressive models that have been used to predict human motion<sup>13,28</sup>) may be used to encode the temporal sequence of muscle features and enable the prediction of transition points between ambulation modes.

Proximal neuromuscular disorders or dystrophy may accompany distal joint disabilities, and prediction accuracy may reduce for amputee subjects due to their decreased ability to contract the muscles in the residual limb. However, it has been reported that the predictability of gait initiation is mostly consistent between the amputee and able-bodied subjects.<sup>49</sup> Extending the results of the present work to amputee subjects may be possible through simulating bilateral knee extension/flexion by contracting the muscles in both thighs at the same time. In the present study, the predictability of movement was only evaluated using ultrasound features of the RF muscle. There have been some reports that other muscles in the upper leg (e.g. tensor fasciae latae muscle) may have greater time precedence to gait initiation.<sup>48</sup> Therefore, it would be meaningful to study the time-precedence of ultrasound features measured from additional muscles.

In conclusion, the feasibility of using ultrasound features of RF muscle to predict the kinematics of upcoming knee motion was demonstrated in the present study. Statistical analysis revealed that there was a time window between 133 and 142 ms, where a *statistically* and *clinically* reliable prediction of joint motion can be achieved. The results motivate the future work toward implementing an ultrasound-based sensing interface for the control of lower-limb assistive devices. Future research to investigate the predictability of the joint motion during dynamic tasks could unveil the feasibility of predicting the critical points during ambulation, such as the transition between ambulation modes. Reliable prediction of the joint motion will not

only improve the control outcomes of assistive devices but also contributes to an intuitive and seamless integration of these devices with the human body and the environment, restoring the natural function of individuals.

## ACKNOWLEDGMENTS

This project was supported by discretionary funds and NSF grant 1925343 of NPF, as well as funding from KH: NIH grant K25EB017222, and NSF grant 1925343.

## REFERENCES

- <sup>1</sup>Ageberg, E., J. Flenhagen, and J. Ljung. Test-retest reliability of knee kinesthesia in healthy adults. *BMC Musculoskelet. Disord.* 8:57, 2007.
- <sup>2</sup>Akhlaghi, N., C. A. Baker, M. Lahlou, H. Zafar, K. G. Murthy, H. S. Rangwala, J. Kosecka, W. M. Joiner, J. J. Pancrazio, and S. Sikdar. Real-time classification of hand motions using ultrasound imaging of forearm muscles. *IEEE Trans. Biomed. Eng.* 63:1687–1698, 2016.
- <sup>3</sup>AlMohimeed, I., and Y. Ono. Ultrasound measurement of skeletal muscle contractile parameters using flexible and wearable single-element ultrasonic sensor. *Sensors* 20:3616, 2020.
- <sup>4</sup>Barrack, R. L., H. B. Skinner, and S. L. Buckley. Proprioception in the anterior cruciate deficient knee. *Am. J. Sports Med.* 17:1–6, 1989.
- <sup>5</sup>Begovic, H., G.-Q. Zhou, T. Li, Y. Wang, and Y.-P. Zheng. Detection of the electromechanical delay and its components during voluntary isometric contraction of the quadriceps femoris muscle. *Front. Physiol.* 5:494, 2014.
- <sup>6</sup>Cooper, R. A., and R. Cooper. Rehabilitation engineering: a perspective on the past 40-years and thoughts for the future. *Med. Eng. Phys.* 72:3–12, 2019.
- <sup>7</sup>Dai, C., Y. Cao, and X. Hu. Prediction of individual finger forces based on decoded motoneuron activities. *Ann. Biomed. Eng.* 47:1357–1368, 2019.
- <sup>8</sup>Dhawan, A. S., B. Mukherjee, S. Patwardhan, N. Akhlaghi, G. Diao, G. Levay, R. Holley, W. M. Joiner, M. Harris-Love, and S. Sikdar. Proprioceptive sonomyographic control: a novel method for intuitive and proportional control of multiple degrees-of-freedom for individuals with upper extremity limb loss. *Sci. Rep.* 9:1–15, 2019.
- <sup>9</sup>Dieterich, A. V., A. Botter, T. M. Vieira, A. Peolsson, F. Petzke, P. Davey, and D. Falla. Spatial variation and inconsistency between estimates of onset of muscle activation from EMG and ultrasound. *Sci. Rep.* 7:42011, 2017.
- <sup>10</sup>Dieterich, A. V., C. M. Pickard, L. E. Deshon, G. R. Strauss, W. Gibson, P. Davey, and J. McKay. M-mode ultrasound used to detect the onset of deep muscle activity. *J. Electromyogr. Kinesiol.* 25:224–231, 2015.
- <sup>11</sup>Dixon, J. R. The international conference on harmonization good clinical practice guideline. *Qual. Assur.* 6:65–74, 1999.
- <sup>12</sup>Elder, G. C., K. Bradbury, and R. Roberts. Variability of fibre type distributions within human muscles. *J. Appl. Physiol.* 53:1473–1480, 1982.
- <sup>13</sup>Farmer, S., B. Silver-Thorn, P. Voglewede, and S. A. Beardsley. Within-socket myoelectric prediction of continuous ankle kinematics for control of a powered transtibial prosthesis. *J. Neural Eng.* 11:056027, 2014.
- <sup>14</sup>Farrell, T. R., and R. F. Weir. The optimal controller delay for myoelectric prostheses. *IEEE Trans. Neural Syst. Rehabil. Eng.* 15:111–118, 2007.
- <sup>15</sup>Fluit, R., E. C. Prinsen, S. Wang, and H. van der Kooij. A comparison of control strategies in commercial and research knee prostheses. *IEEE Trans. Biomed. Eng.* 67:277–290, 2020.
- <sup>16</sup>Fukunaga, T., Y. Kawakami, S. Kuno, K. Funato, and S. Fukashiro. Muscle architecture and function in humans. *J. Biomech.* 30:457–463, 1997.
- <sup>17</sup>Gerardo, C. D., E. Cretu, and R. Rohling. Fabrication and testing of polymer-based capacitive micromachined ultrasound transducers for medical imaging. *Microsyst. Nanoeng.* 4:1–12, 2018.
- <sup>18</sup>Grob, K. R., M. S. Kuster, S. A. Higgins, D. G. Lloyd, and H. Yata. Lack of correlation between different measurements of proprioception in the knee. *J. Bone Joint Surg.* 84:5, 2002.
- <sup>19</sup>Hagberg, K., and R. Bränemark. Consequences of non-vascular trans-femoral amputation: a survey of quality of life, prosthetic use and problems. *Prosthet. Orthot. Int.* 25:186–194, 2001.
- <sup>20</sup>He, J., H. Luo, J. Jia, J. T. W. Yeow, and N. Jiang. Wrist and finger gesture recognition with single-element ultrasound signals: a comparison with single-channel surface electromyogram. *IEEE Trans. Biomed. Eng.* 66:1277–1284, 2019.
- <sup>21</sup>Henneman, E., G. Somjen, and D. O. Carpenter. Functional significance of cell size in spinal motoneurons. *J. Neurophysiol.* 28:560–580, 1965.
- <sup>22</sup>Hodson-Tole, E. F., and J. M. Wakeling. Motor unit recruitment for dynamic tasks: current understanding and future directions. *J. Comp. Physiol. B* 179:57–66, 2009.
- <sup>23</sup>Howell D. C. *Statistical Methods for Psychology*. Boston: Cengage Learning, 2009.
- <sup>24</sup>Jahanandish, M. H., N. P. Fey, and K. Hoyt. Lower limb motion estimation using ultrasound imaging: a framework for assistive device control. *IEEE J. Biomed. Health Inform.* 23:2505–2514, 2019.
- <sup>25</sup>Jahanandish M. H., N. P. Fey and K. Hoyt. Prediction of distal lower-limb motion using ultrasound-derived features of proximal skeletal muscle. In: 2019 IEEE 16th International Conference on Rehabilitation Robotics (ICORR), 2019, pp. 71–76.
- <sup>26</sup>Jahanandish M. H., K. G. Rabe, N. P. Fey and K. Hoyt. Gait phase identification during level, incline and decline ambulation tasks using portable sonomyographic sensing. In: 2019 IEEE 16th International Conference on Rehabilitation Robotics (ICORR), 2019, pp. 988–993.
- <sup>27</sup>Johnson, M. A., J. Polgar, D. Weightman, and D. Appleton. Data on the distribution of fibre types in thirty-six human muscles: an autopsy study. *J. Neurol. Sci.* 18:111–129, 1973.
- <sup>28</sup>Koch P., H. Phan, M. Maass, F. Katzberg and A. Mertins. Recurrent neural network based early prediction of future hand movements. In: 2018 40th Annual International Conference of the IEEE Engineering in Medicine and Biology Society (EMBC) IEEE, 2018, pp. 4710–4713.

<sup>29</sup>Li J., F. Kong, X. Gao, Y. Shen and S. Gao. Prospective randomized comparison of knee stability and proprioception for posterior cruciate ligament reconstruction with autograft, hybrid graft, and  $\gamma$ -irradiated allograft. *Arthroscopy* 32: 2548–2555, 2016.

<sup>30</sup>Lopata, R. G. P., J. P. van Dijk, S. Pillen, M. M. Nillesen, H. Maas, J. M. Thijssen, D. F. Stegeman, and C. L. de Korte. Dynamic imaging of skeletal muscle contraction in three orthogonal directions. *J. Appl. Physiol.* 109:906–915, 2010.

<sup>31</sup>Marcucci, L., M. Bondi, G. Randazzo, C. Reggiani, A. N. Natali, and P. G. Pavan. Fibre and extracellular matrix contributions to passive forces in human skeletal muscles: an experimental based constitutive law for numerical modelling of the passive element in the classical Hill-type three element model. *PLoS ONE* 14:e0224232, 2019.

<sup>32</sup>Molenberghs, G., and G. Verbeke. A review on linear mixed models for longitudinal data, possibly subject to dropout. *Stat. Model.* 1:235–269, 2001.

<sup>33</sup>National Academies of S. and Medicine. The Promise of Assistive Technology to Enhance Activity and Work Participation. Washington: National Academies Press, 2017.

<sup>34</sup>Pataky, T. C. Generalized n-dimensional biomechanical field analysis using statistical parametric mapping. *J. Biomech.* 43:1976–1982, 2010.

<sup>35</sup>Penny W. D., K. J. Friston, J. T. Ashburner, S. J. Kiebel and T. E. Nichols. Statistical Parametric Mapping: The Analysis of Functional Brain Images. New York: Elsevier, 2011.

<sup>36</sup>Qiu, S., J. Feng, J. Xu, R. Xu, X. Zhao, P. Zhou, H. Qi, L. Zhang, and D. Ming. Sonomography analysis on thickness of skeletal muscle during dynamic contraction induced by neuromuscular electrical stimulation: a pilot study. *IEEE Trans. Neural Syst. Rehabil. Eng.* 25:62–70, 2017.

<sup>37</sup>Rabe K. G., M. H. Jahanandish, K. Hoyt and N. P. Fey. Use of sonomyographic sensing to estimate knee angular velocity during varying modes of ambulation. In: 2020 42nd Annual International Conference of the IEEE Engineering in Medicine and Biology Society (EMBC), 2020.

<sup>38</sup>Rabe K. G., M. H. Jahanandish, K. Hoyt and N. P. Fey. Use of sonomyography for continuous estimation of hip, knee and ankle moments during multiple ambulation tasks. In: 2020 8th IEEE RAS/EMBS International Conference on Biomedical Robotics and Biomechatronics (BioRob), 2020.

<sup>39</sup>Rasmussen C. E. Gaussian Processes in Machine Learning. New York: Springer, 2003, pp. 63–71.

<sup>40</sup>Reider B., M. A. Arcand, L. H. Diehl, K. Mroczek, A. Abulencia, C. C. Stroud, M. Palm, J. Gilbertson and P. Staszak. Proprioception of the knee before and after anterior cruciate ligament reconstruction. *Arthroscopy* 19: 2–12, 2003.

<sup>41</sup>Simon, A. M., K. A. Ingraham, J. A. Spanias, A. J. Young, S. B. Finucane, E. G. Halsne, and L. J. Hargrove. Delaying ambulation mode transition decisions improves accuracy of a flexible control system for powered knee-ankle prosthesis. *IEEE Trans. Neural Syst. Rehabil. Eng.* 25:1164–1171, 2017.

<sup>42</sup>Smith, L. H., L. J. Hargrove, B. A. Lock, and T. A. Kuijken. Determining the optimal window length for pattern recognition-based myoelectric control: balancing the competing effects of classification error and controller delay. *IEEE Trans. Neural Syst. Rehabil. Eng.* 19:186–192, 2011.

<sup>43</sup>Tidball J. and T. Daniel. Myotendinous junctions of tonic muscle cells: structure and loading. *Cell Tissue Res* 245:1986.

<sup>44</sup>Voloshina A. S. and S. H. Collins. Lower limb active prosthetic systems—Overview. In: Wearable Robotics, edited by J. Rosen and P. W. Ferguson. New York: Academic Press, 2020, pp. 469–486.

<sup>45</sup>Wakeling, J. M. Motor units are recruited in a task-dependent fashion during locomotion. *J. Exp. Biol.* 207:3883–3890, 2004.

<sup>46</sup>Wakeling, J. M., K. Uehli, and A. I. Rozitis. Muscle fibre recruitment can respond to the mechanics of the muscle contraction. *J. R. Soc. Interface* 3:533–544, 2006.

<sup>47</sup>Wei, P.-N., R. Xie, R. Tang, C. Li, J. Kim, and M. Wu. sEMG based gait phase recognition for children with spastic cerebral palsy. *Ann. Biomed. Eng.* 47:223–230, 2019.

<sup>48</sup>Wentink, E. C., S. I. Beijen, H. J. Hermens, J. S. Rietman, and P. H. Veltink. Intention detection of gait initiation using EMG and kinematic data. *Gait Posture* 37:223–228, 2013.

<sup>49</sup>Wentink, E. C., V. G. H. Schut, E. C. Prinsen, J. S. Rietman, and P. H. Veltink. Detection of the onset of gait initiation using kinematic sensors and EMG in trans-femoral amputees. *Gait Posture* 39:391–396, 2014.

<sup>50</sup>World Health Organization. *World report on disability 2011*. World Health Organization, 2011.

<sup>51</sup>Yang X., J. Yan and H. Liu. Comparative analysis of wearable a-mode ultrasound and sEMG for muscle-computer interface. *IEEE Trans. Biomed. Eng.* 1–1, 2019.

<sup>52</sup>Zhang F., M. Liu and H. Huang. Investigation of timing to switch control mode in powered knee prostheses during task transitions. *PLoS ONE* 10: 2015.

<sup>53</sup>Zhang, Q., K. Kim, and N. Sharma. Prediction of ankle dorsiflexion moment by combined ultrasound sonography and electromyography. *IEEE Trans. Neural Syst. Rehabil. Eng.* 28:318–327, 2020.

**Publisher's Note** Springer Nature remains neutral with regard to jurisdictional claims in published maps and institutional affiliations.